Experimental report

28/02/2025

Proposal: CRG-3123 **Council:** 4/2024

Title: Exploring the magnetoelastic transition in Fe49Rh51 through neutron first-order reverse curves under magnetic field

Research area:

This proposal is a new proposal

Main proposer: Pablo ALVAREZ

Experimental team: Kenny PADRON ALEMAN
Pablo ALVAREZ

Local contacts: Ines PUENTE ORENCH
Stanislav SAVVIN

Samples: Fe49.5Rh50.5

Instrument	Requested days	Allocated days	From	To
D1B	3	0		
XTREMED	3	3	31/05/2024	03/06/2024

Abstract:

Report XtremeD Proposal CRG-D1B-23-564

The magnetocaloric (MC) effect occurs due to the coupling between the magnetic and thermal properties of a material. $Fe_{100-x}Rh_x$ alloys with $48 \leq x \leq 52$ at. % are MC materials of significant interest due to their sharp changes in magnetization and the largest adiabatic changes in temperature reported to date [1]. Within this composition range, the Fe-Rh alloys crystallize in the CsCl-type crystal structure (B2 structure) and undergo a temperature- and magnetically-driven magnetostructural first-order phase transition (FOPT). The features of this transition are consequence of the competition between the antiferromagnetic (AFM) and ferromagnetic (FM) phases in the context of a complex nucleation process [2].

The analysis of the magnetization through temperature first order reverse curve (T-FORC) has demonstrated that the alloy with composition $Fe_{49}Rh_{51}$exhibits homogeneous nucleation sites, likely associated with abundant and fast nucleation promoted by the Rh-excess atoms. Analogously to T-FORC, a first-order reverse neutron thermo-diffraction (n-FORC) experiment was carried out in a previous beamtime. From the analysis of the n-FORC diagrams, it is clear the strong coupling of the structural and magnetic transformations. Furthermore, another results obtained through neutron diffraction experiments without applied magnetic field suggest that both structures resemble a hand-to-hand evolution throughout the phase transformation, as well as a phase arrest of the AFM phase was identified, in 70 K after and before of the first order phase transformation, suggesting two kinds of dynamics of the transition, one during the FOTP and the other in the T-range of the phase arrest.

In this beamtime we intended scrutinize the first order phase transformation through neutron diffraction experiments of this same alloy when it is isothermally induced by applied magnetic fields and temperature-induced at a fixed magnetic field. We planned to study the effect of the magnetic field on the dynamic of the phase transition, the AFM phase arrest, and on the spin-lattice coupling.

The wavelength used in our experiments was $\lambda = 2.44$ Å. For the study of the magnetic field-induced transition, neutron diffraction experiments were conducted isothermally across the AFM-FM transition at fixed values of $\mu_0 H$ while increasing the field from 0 to 10 T. For the FM-AFM transition, patterns were collected at fixed values of $\mu_0 H$ as the field was decreased from 10 to 0 T. This process was repeated at different temperatures: 265, 275, 285, and 294 K. In the case of the temperature-induced transition at an applied magnetic field, $\mu_0 H$ was fixed at 8 T and the thermo-patterns were accumulated each 2 min in T-ramps of 1 K/min, in the temperature range of 100-294 K in heating, and 294-100 K in cooling. Furthermore, temperature first order reverse curve of neutron diffraction (n-FORC (ND)) at 8 T applied magnetic field was calculated in the FM-AFM transition to fingerprint and study the coupling of the magnetic and structural transformation.

Fig. 1. (a) and (b) display the neutron diffraction (ND) patterns at 294 K under 0 T and 10 T magnetic fields, along with their corresponding Rietveld refinements. At 0 T, the sample is fully antiferromagnetic (AFM), while at 10 T, the sample predominantly is ferromagnetic (FM), though a small fraction of the AFM phase remains. Fig. 2(a) displays a contour map of the higher intensity

nuclear/FM peak of the neutron diffraction patterns, collected at a constant temperature of T = 294 K while increasing $\mu_0 H$. The first-order phase transition is observed in the range of 5–5.5 T. The higher AFM intensity peak during the increasing $\mu_0 H$ regime (Fig. 1(b)) shows that AFM order persists in the alloy, even 4.5 T after the first-order phase transition (FOPT), and remains up to the highest field applied in our experiment, 10 T. In the decreasing $\mu_0 H$ regime (Fig. 1(c)), AFM order is also observed before the FM-AFM transition.

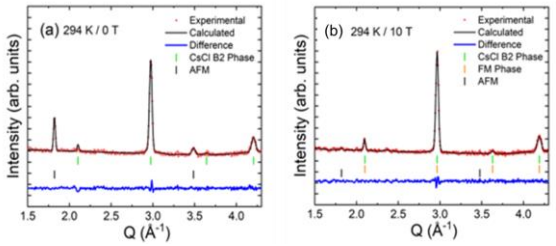

Fig. 1. Neutron diffraction patterns at 294 K and the Rietveld refinement under an applied magnetic field of (a) 0 T and (b) 10 T.

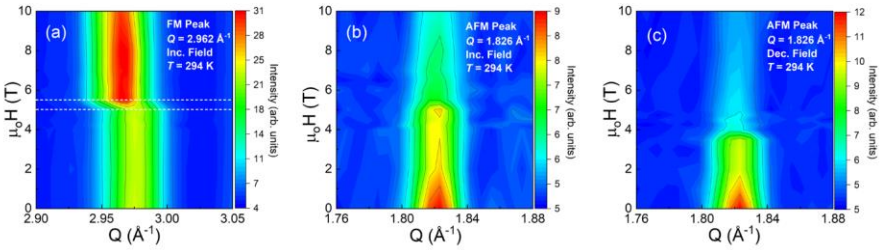

Fig. 2. Contour maps of the (a) high-intensity FM/nuclear peak of the neutron diffraction patterns at 294 K, and (b) high-intensity AFM peak with the field increasing from 0 to 10 T (c) Contour map of the high-intensity AFM peak as the field decreases from 10 to 0 T. The white horizontal dashed lines in (a) indicate the magnetic-field-induced AFM-FM first-order phase transition.

The evolution of lattice parameter, magnetic moments of the Fe atoms, and phase fraction were obtained from Rietveld analysis of the neutron diffraction patterns. Fig. 3 shows the evolution of the lattice parameter, magnetic moments, and phase fraction for the 294 K isothermal for magnetic field applied from 0 to 10 T. Furthermore, from the evolution of the lattice parameter in each isothermal curve (Fig. 4) we obtained the critic magnetic field to induce the transition (Fig. 5), $\mu_0 H_c$ = -9 K/T, and from the n-FORC distribution of the lattice parameter and phase fraction of the AFM phase is inferred that both the structural and magnetic transformation occurs simultaneously under a magnetic field as well.

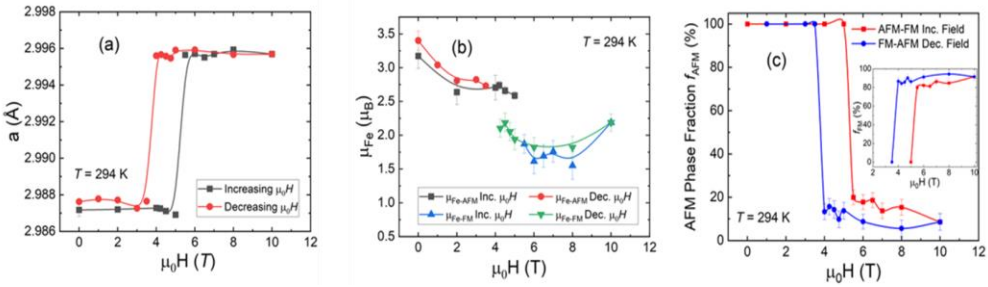

Fig. 3. Isothermal evolution at 294 K increasing the magnetic field from 0 to10 T, and decreasing it from 10 to 0 T (a) cell parameter a, (b) magnetic moment of the Fe atoms in the AFM and FM phases, and (c) evolution of the AFM phase fraction (inset: evolution of the FM phase fraction) during the first order phase transition.

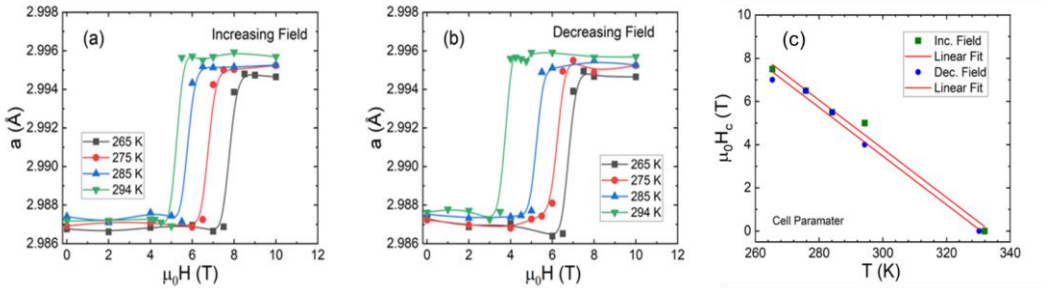

Fig. 4. (a) Evolution of the lattice parameter during the magnetic-field-induced AFM↔FM first-order phase transition at 265, 275, 285, and 294 K, as the magnetic field is increased from 0 to 10 T, and (b) while decreasing the magnetic field from 10 to 0 T. (c) Lineal dependence of the critic magnetic field needed to induce the AFM↔FM first order phase transformation at constant temperature

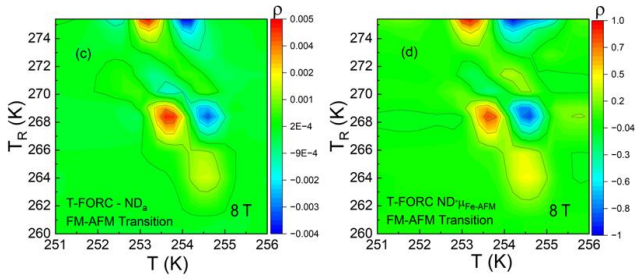

Fig. 8. n-FORC distribution linked to the FM-AFM transition under an applied 8 T magnetic field in terms of the temperature evolution of the cell parameter *a* (a), and the Fe magnetic moment in the AFM state (b).

These results, combined with the findings from the AFM↔FM transition induced without an applied magnetic field, provide a broader perspective and offer new insights into the underlying mechanisms driving the first-order phase transition in these alloys.

References

[1] F. de Bergevin, L. Muldawer, Compt. Rend. 252 (1961) 1347.
[2] D.J. Keavney et al., 8:1. 8 (2018) 1–7.